Acta Cryst. (1971). B**27**, 1037

Structural Systematics in the Binary System Ta_2O_5–WO_3. V. The Structure of the Low-Temperature Form of Tantalum Oxide *L*-Ta_2O_5

BY N. C. STEPHENSON* AND R. S. ROTH

National Bureau of Standards, Washington, D.C. 20234, USA

(*Received* 9 *March* 1970 *and in revised form* 27 *July* 1970)

The orthogonal unit cell of the compound *L*-Ta_2O_5 has dimensions $a=6{\cdot}198$, $b=40{\cdot}29$, $c=3{\cdot}888$ Å and contains 11 formula units. The structure was solved in projection from the Patterson function and refined to a conventional *R* value of 0·088 using full-matrix least-squares methods. The metal atoms are arranged in sheets and are surrounded by oxygen atoms which form either distorted octahedral or pentagonal bipyramidal coordination polyhedra. The structure contains, on the average, three distortion planes per unit cell. These are statistically distributed over four sites, thereby giving the average unit cell a higher symmetry than the real unit cell. The thermal equilibration of the compound, involving detectable structural changes, is discussed in terms of the migration of distortion planes.

Introduction

Pure Ta_2O_5 has at least two structurally distinct polymorphs, with a reversible phase transition occurring at about 1360°C. The high-temperature form was first reported by Lagergren & Magnéli (1952) and was shown to undergo several small symmetry changes when heated and cooled (Laves & Petter, 1964; Waring & Roth, 1968). A large number of X-ray diffraction powder patterns of the low-temperature form of Ta_2O_5 have been published. Although all the published patterns are similar with respect to the strong (substructure) lines, there is little or no agreement as to the positions of the weaker (superstructure) lines. Moser (1965) has divided the low temperature form into four subdivisions based on the position of one of the more sensitive superstructure peaks called the *C* line. Roth & Waring (1971) have shown that the variable position of the superstructure lines depends on the exact nature of the heat treatment and is, at least partially, reversible and therefore represents an equilibrium condition. Under heat treatment the *C* line was found to move from lower to higher *d* values with increasing temperature with the largest value occurring only when the specimen had been quenched from just below or (for heat treatments of short deviation) from just above the phase transition temperature. Very small single crystals of Ta_2O_5 have been prepared in this structure type (with the *C* line at the largest possible *d* spacing) by successive heating of a specimen at 1700°C for 20 hours, 1225°C for two weeks, 1325°C for two weeks and 1350°C for two weeks, with quenching to room temperature after each heat treatment.

Lehovic (1964) described the structure of the tantalum oxide subcell with the tantalum atoms near positions (000, $\frac{1}{2}\frac{1}{2}0$), two oxygen atoms at about ($00\frac{1}{2}$, $\frac{1}{2}\frac{1}{2}\frac{1}{2}$) and the other three oxygen atoms in the same plane as the tantalum atoms. The positions of these latter three oxygens in the (001) plane were described as 'uncertain'.

* Permanent address: School of Chemistry, University of New South Wales, Sydney, Australia.

Experimental

Crystals of *L*-Ta_2O_5 were smaller than any previously examined in the Ta_2O_5–WO_3 system. A crystal, larger than average, was eventually mounted on a fibre of glass wool and oriented about the *a* axis. This crystal, which was near spherical in shape with an average radius of 0·010 mm, was used to collect data on a General Electric single-crystal orienter. Unit-cell dimensions were obtained using a Philips powder diffractometer with Cu $K\alpha$ radiation. The crystal data are: *L*-Ta_2O_5, $M=441{\cdot}75$; $a=6{\cdot}198$ (5), $b=40{\cdot}290$ (33), $c=3{\cdot}888$ (5) Å; $V=970{\cdot}9$ Å^3, $Z=11$, $D_c=8{\cdot}31$ g.cm^{-3}.

Intensities were measured by the 2θ-scan method using Mo $K\alpha$ radiation. Because of the large *b* axis dimension it was necessary to critically determine the *smallest* scan range that still completely covered each reflection and also to use a 0·2° slit immediately in front of the scintillation counter window to minimize peak overlap. The orientation of the crystal was such that the slit was used in a horizontal position, *i.e.* in the equatorial plane of the diffractometer. The rate of scanning was 1°.min^{-1} and the scan range (SR) was calculated using the equation $\mathrm{SR}=1{\cdot}5+0{\cdot}8\tan\theta$. The backgrounds were measured for 60 seconds at $2\theta\pm\frac{1}{2}$ SR. The intensities of three standard reflections, measured periodically with the data, were found to hold constant to within 5%. A standard deviation (σ) was calculated for each intensity and if the net number of counts did not exceed 2σ the reflection was considered as a 'less than' and its intensity was set equal to 2σ. In the 2θ angle range 0–100° a unique set of 938 *hk*0 reflections was recorded, of which 686 were labelled as 'less thans'. Lorentz–polarization but not absorption corrections ($\mu R=0{\cdot}65$) were applied to these data to yield the set of observed structure factors listed in Table 1. Atomic scattering curves and computer programs were the same as described previously (Stephenson & Roth, 1971*a*).

Determination and refinement of the structure

The determination of the structure of L-Ta_2O_5 was similar to that of $Ta_{30}W_2O_{81}$ (Stephenson & Roth,

Table 1. *Observed and calculated structure factors.*

Unobserved data are marked with L.

H	K	L	GRP		FO	FC
0	2	0	1	L	115	14
0	3	0	1	L	45	13
0	4	0	1	L	44	11
0	5	0	1	L	46	13
0	6	0	1	L	48	8
0	7	0	1	L	51	18
0	8	0	1		89	106
0	9	0	1	L	54	14
0	10	0	1	L	53	9
0	11	0	1	L	54	7
0	12	0	1	L	74	68
0	13	0	1	L	70	24
0	14	0	1		223	210
0	15	0	1	L	68	18
0	16	0	1	L	63	27
0	17	0	1	L	67	71
0	18	0	1	L	70	45
0	19	0	1	L	102	6
0	20	0	1		137	56
0	21	0	1	L	150	26
0	22	0	1		1028	1157
0	23	0	1	L	158	73
0	24	0	1	L	106	21
0	25	0	1	L	105	41
0	26	0	1	L	104	27
0	27	0	1	L	103	69
0	28	0	1	L	99	61
0	29	0	1	L	105	10
0	30	0	1		269	262
0	31	0	1	L	109	49
0	32	0	1		122	45
0	33	0	1	L	92	90
0	34	0	1	L	86	59
0	35	0	1	L	109	92
0	36	0	1		359	331
0	37	0	1	L	117	58
0	38	0	1	L	90	95
0	39	0	1		135	73
0	40	0	1	L	103	48
0	41	0	1	L	90	90
0	42	0	1	L	91	26
0	43	0	1	L	131	13
0	44	0	1		542	511
0	45	0	1	L	155	83
0	46	0	1	L	96	23
0	47	0	1	L	98	55
0	48	0	1	L	93	24
0	49	0	1	L	95	54
0	50	0	1	L	96	111
0	51	0	1	L	112	24
0	52	0	1		231	225
0	53	0	1	L	118	82
0	54	0	1	L	91	19
0	55	0	1	L	94	52
0	56	0	1	L	90	78
0	57	0	1	L	107	28
0	58	0	1		206	230
0	59	0	1	L	118	83
0	60	0	1	L	99	99
0	61	0	1	L	97	47
0	62	0	1	L	91	41
0	63	0	1	L	92	44
0	64	0	1	L	92	28
0	65	0	1	L	99	29
0	66	0	1		193	191
0	67	0	1	L	121	36
0	68	0	1	L	93	18
0	69	0	1	L	91	39
0	70	0	1	L	91	25
0	71	0	1	L	98	28
0	72	0	1		139	129
0	73	0	1	L	101	47
0	74	0	1	L	103	128
0	75	0	1	L	108	74
0	76	0	1	L	89	8
0	77	0	1	L	88	90
0	78	0	1	L	92	66
0	79	0	1	L	95	2
0	80	0	1	L	101	115
1	80	0	1	L	90	30
1	79	0	1	L	91	16
1	78	0	1	L	110	19
1	77	0	1	L	104	44
1	76	0	1	L	92	65
1	75	0	1	L	84	26
1	74	0	1	L	82	41
1	73	0	1	L	83	45
1	72	0	1	L	84	29
1	71	0	1	L	91	86
1	70	0	1	L	109	96
1	69	0	1		152	157
1	68	0	1	L	79	55
1	67	0	1	L	76	63
1	66	0	1	L	77	48
1	65	0	1	L	77	13
1	64	0	1	L	113	94
1	63	0	1		217	181
1	62	0	1	L	102	55
1	61	0	1		191	126
1	60	0	1	L	83	30
1	59	0	1	L	75	38
1	58	0	1	L	78	44
1	57	0	1	L	82	11
1	56	0	1	L	132	69
1	54	0	1	L	92	104
1	53	0	1	L	73	34
1	52	0	1	L	63	40
1	51	0	1	L	64	56
1	50	0	1	L	76	60
1	49	0	1	L	83	83
1	48	0	1	L	119	109
1	47	0	1		260	250
1	46	0	1	L	86	80
1	45	0	1	L	64	61
1	44	0	1	L	59	46
1	43	0	1	L	70	23
1	42	0	1	L	119	79
1	41	0	1		298	284
1	40	0	1	L	83	103
1	39	0	1		96	87
1	38	0	1	L	64	58
1	37	0	1	L	60	32
1	36	0	1	L	61	52
1	35	0	1	L	65	19
1	34	0	1	L	150	110
1	33	0	1		718	676
1	32	0	1	L	85	140
1	31	0	1	L	64	53
1	30	0	1	L	61	30
1	29	0	1	L	61	41
1	28	0	1	L	60	75
1	27	0	1	L	65	51
1	25	0	1		295	260
1	24	0	1		59	64
1	23	0	1	L	56	34
1	22	0	1	L	56	29
1	21	0	1	L	57	15
1	20	0	1	L	64	33
1	19	0	1		354	303
1	18	0	1		232	220
1	17	0	1	L	55	17
1	16	0	1	L	55	57
1	15	0	1	L	53	9
1	14	0	1	L	53	43
1	13	0	1	L	55	4
1	12	0	1		133	197
1	11	0	1		894	1215
1	10	0	1		217	186
1	9	0	1	L	53	33
1	8	0	1	L	52	10
1	7	0	1	L	51	23
1	6	0	1	L	51	20
1	5	0	1	L	51	15

H	K	L	GRP		FO	FC
1	4	0	1		110	193
1	3	0	1	L	50	40
1	2	0	1	L	48	7
1	1	0	1	L	48	21
1	0	0	1	L	48	32
2	0	0	1		1063	1075
2	1	0	1		338	350
2	2	0	1	L	54	49
2	3	0	1	L	53	25
2	4	0	1	L	54	20
2	5	0	1	L	54	16
2	6	0	1		87	78
2	7	0	1		290	221
2	8	0	1		263	229
2	9	0	1	L	55	56
2	10	0	1	L	54	30
2	11	0	1	L	52	33
2	12	0	1	L	52	36
2	13	0	1	L	55	5
2	14	0	1		190	124
2	15	0	1		274	229
2	16	0	1		56	34
2	17	0	1	L	53	51
2	18	0	1	L	53	35
2	19	0	1	L	52	15
2	20	0	1		78	83
2	21	0	1		364	363
2	22	0	1		756	799
2	23	0	1		240	241
2	24	0	1	L	59	11
2	25	0	1		56	48
2	26	0	1	L	59	47
2	27	0	1	L	96	89
2	28	0	1	L	58	15
2	29	0	1		155	146
2	30	0	1		373	328
2	31	0	1		66	68
2	32	0	1	L	60	34
2	33	0	1	L	59	50
2	34	0	1	L	58	54
2	35	0	1		71	62
2	36	0	1		249	214
2	37	0	1		159	132
2	38	0	1	L	67	55
2	39	0	1	L	56	57
2	40	0	1	L	54	53
2	41	0	1	L	58	21
2	42	0	1	L	62	82
2	43	0	1		289	291
2	44	0	1		411	376
2	45	0	1	L	122	132
2	46	0	1	L	73	24
2	47	0	1	L	64	51
2	48	0	1	L	66	59
2	49	0	1	L	68	39
2	50	0	1		98	85
2	51	0	1	L	82	81
2	52	0	1		259	231
2	53	0	1	L	113	77
2	54	0	1	L	71	35
2	55	0	1	L	65	58
2	56	0	1	L	64	70
2	57	0	1		84	84
2	58	0	1		223	175
2	59	0	1	L	106	105
2	60	0	1	L	85	83
2	61	0	1	L	78	26
2	62	0	1	L	72	49
2	63	0	1	L	74	30
2	64	0	1	L	76	46
2	65	0	1		152	136
2	66	0	1	L	118	137
2	67	0	1	L	114	57
2	68	0	1	L	82	26
2	69	0	1	L	80	40
2	70	0	1	L	78	46
2	71	0	1	L	79	33
2	73	0	1	L	97	48
2	74	0	1		128	121
2	75	0	1	L	109	74
2	76	0	1	L	84	35
2	77	0	1		84	56
2	78	0	1	L	79	63
2	79	0	1	L	92	74
2	80	0	1	L	99	103
3	80	0	1	L	88	27
3	79	0	1	L	87	23
3	78	0	1	L	84	34
3	77	0	1	L	109	70
3	76	0	1		136	132
3	75	0	1	L	83	45
3	74	0	1	L	76	21
3	73	0	1	L	77	40
3	72	0	1	L	77	17
3	71	0	1	L	89	73
3	70	0	1	L	86	89
3	69	0	1	L	85	88
3	68	0	1	L	86	93
3	66	0	1	L	84	67
3	65	0	1	L	80	44
3	64	0	1	L	108	64
3	63	0	1		161	183
3	62	0	1	L	71	75
3	61	0	1	L	72	28
3	57	0	1	L	70	19
3	56	0	1		101	102
3	55	0	1		192	181
3	54	0	1		257	236
3	53	0	1		105	89
3	52	0	1	L	67	41
3	51	0	1	L	64	54
3	50	0	1	L	67	41
3	49	0	1		69	65
3	48	0	1		144	135
3	47	0	1		109	119
3	46	0	1	L	70	86
3	45	0	1	L	65	72
3	44	0	1	L	59	67
3	43	0	1	L	60	47
3	42	0	1		104	82
3	41	0	1		343	308
3	40	0	1		148	154
3	39	0	1	L	65	52
3	38	0	1	L	54	10
3	37	0	1	L	56	52
3	36	0	1	L	53	66
3	35	0	1	L	60	25
3	34	0	1		189	208
3	32	0	1		402	375
3	31	0	1		161	193
3	30	0	1	L	60	48
3	29	0	1	L	59	67
3	28	0	1	L	59	60
3	27	0	1	L	57	54
3	26	0	1		257	237
3	25	0	1	L	59	43
3	24	0	1		58	45
3	23	0	1	L	55	46
3	22	0	1	L	56	31
3	21	0	1	L	56	46
3	20	0	1		101	99
3	19	0	1		376	368
3	18	0	1		275	286
3	17	0	1		151	192
3	16	0	1	L	54	31
3	15	0	1	L	53	31
3	14	0	1	L	54	42
3	13	0	1		66	61
3	12	0	1		436	373
3	11	0	1		814	844
3	10	0	1		486	467
3	9	0	1	L	54	43
3	7	0	1	L	53	35

H	K	L	GRP		FO	FC
3	6	0	1	L	53	98
3	5	0	1		189	163
3	4	0	1		391	361
3	3	0	1		237	243
3	2	0	1		69	74
3	1	0	1	L	54	19
3	0	0	1	L	73	2
4	0	0	1		668	519
4	1	0	1		370	396
4	2	0	1		104	102
4	3	0	1	L	53	23
4	5	0	1	L	55	43
4	6	0	1		226	205
4	7	0	1		226	257
4	8	0	1		382	381
4	9	0	1		163	139
4	10	0	1	L	55	55
4	11	0	1	L	56	42
4	12	0	1	L	56	38
4	13	0	1	L	64	70
4	14	0	1		157	177
4	15	0	1		161	196
4	16	0	1		103	113
4	17	0	1	L	58	53
4	18	0	1	L	57	46
4	19	0	1	L	58	65
4	20	0	1		165	152
4	21	0	1		378	353
4	22	0	1		413	376
4	23	0	1		199	210
4	24	0	1	L	64	40
4	25	0	1	L	58	65
4	26	0	1	L	55	40
4	27	0	1	L	60	31
4	28	0	1		154	152
4	29	0	1		179	188
4	30	0	1		427	373
4	31	0	1		189	132
4	32	0	1	L	62	49
4	33	0	1	L	60	62
4	34	0	1	L	63	31
4	35	0	1		84	76
4	36	0	1	L	62	12
4	37	0	1		131	136
4	38	0	1	L	56	56
4	39	0	1	L	60	44
4	40	0	1	L	64	59
4	41	0	1		81	71
4	42	0	1		164	150
4	43	0	1		324	274
4	44	0	1		202	180
4	45	0	1		101	115
4	46	0	1	L	65	12
4	47	0	1	L	64	68
4	48	0	1	L	62	65
4	49	0	1	L	64	24
4	50	0	1		89	50
4	51	0	1		94	85
4	52	0	1		263	238
4	53	0	1		133	103
4	54	0	1	L	71	52
4	55	0	1	L	75	73
4	56	0	1		78	70
4	57	0	1		117	100
4	58	0	1	L	71	51
4	59	0	1		94	92
4	60	0	1	L	74	69
4	61	0	1	L	75	23
4	62	0	1	L	74	49
4	63	0	1	L	76	55
4	64	0	1		115	98
4	65	0	1		230	176
4	66	0	1	L	81	85
4	67	0	1	L	76	57
4	68	0	1	L	77	23
4	69	0	1	L	82	46
4	70	0	1	L	74	50
4	71	0	1	L	77	45
4	72	0	1	L	84	9
4	73	0	1	L	82	46
4	74	0	1		126	113
4	75	0	1	L	106	68
4	76	0	1	L	90	47
4	77	0	1	L	86	74
4	78	0	1	L	89	88
4	79	0	1	L	96	90
4	80	0	1	L	85	66
5	80	0	1	L	85	45
5	79	0	1	L	82	14
5	78	0	1	L	88	45
5	77	0	1	L	85	73
5	76	0	1	L	105	124
5	75	0	1	L	103	107
5	74	0	1	L	81	54
5	73	0	1	L	82	39
5	72	0	1	L	81	24
5	71	0	1	L	81	78
5	70	0	1	L	87	62
5	69	0	1	L	81	58
5	68	0	1	L	86	87
5	67	0	1	L	79	82
5	66	0	1	L	73	76
5	65	0	1	L	84	58
5	64	0	1	L	93	78
5	63	0	1	L	107	148
5	62	0	1	L	75	33
5	61	0	1	L	71	39
5	60	0	1	L	73	44
5	59	0	1	L	66	57
5	58	0	1	L	72	57
5	57	0	1	L	73	10
5	56	0	1	L	79	79
5	55	0	1	L	79	89
5	54	0	1		265	209
5	53	0	1		171	165
5	52	0	1	L	74	70
5	51	0	1	L	69	65
5	50	0	1	L	66	15
5	49	0	1	L	64	73
5	48	0	1	L	73	70
5	47	0	1	L	69	38
5	46	0	1	L	66	65
5	45	0	1	L	64	45
5	44	0	1	L	66	68
5	43	0	1	L	69	55
5	42	0	1		138	130
5	41	0	1		346	281
5	40	0	1	L	66	73
5	39	0	1		104	120
5	38	0	1	L	62	44
5	37	0	1	L	61	58
5	36	0	1	L	68	69
5	35	0	1	L	71	34
5	34	0	1		140	146
5	33	0	1		162	164
5	32	0	1		335	303
5	31	0	1		192	183
5	30	0	1	L	60	61
5	29	0	1	L	64	73
5	28	0	1	L	61	48
5	27	0	1		84	96
5	26	0	1		132	103
5	25	0	1		108	106
5	24	0	1		99	81
5	23	0	1	L	56	19
5	22	0	1	L	59	40
5	21	0	1		69	59
5	20	0	1		220	177
5	19	0	1		432	373
5	18	0	1		128	124
5	17	0	1		261	213
5	16	0	1		69	60
5	15	0	1	L	59	17

H	K	L	GRP		FO	FC
5	14	0	1	L	59	51
5	13	0	1		81	90
5	12	0	1		262	238
5	11	0	1		257	264
5	10	0	1		391	323
5	9	0	1		176	158
5	8	0	1	L	59	39
5	7	0	1	L	56	47
5	6	0	1		61	61
5	5	0	1		208	179
5	4	0	1		161	139
5	3	0	1		306	275
5	2	0	1		176	150
5	1	0	1	L	61	64
5	0	0	1	L	85	68
6	0	0	1		292	198
6	1	0	1		250	210
6	2	0	1		106	98
6	3	0	1	L	64	53
6	4	0	1	L	55	34
6	5	0	1		84	105
6	6	0	1		212	197
6	7	0	1		70	74
6	8	0	1		378	397
6	9	0	1		232	222
6	10	0	1	L	61	85
6	11	0	1	L	55	48
6	12	0	1		88	67
6	13	0	1		203	184
6	14	0	1		244	238
6	15	0	1	L	62	48
6	16	0	1		149	132
6	17	0	1	L	60	81
6	18	0	1	L	61	66
6	19	0	1		85	76
6	20	0	1		182	157
6	21	0	1		268	248
6	22	0	1		134	135
6	23	0	1		181	135
6	24	0	1	L	64	56
6	25	0	1		63	65
6	26	0	1	L	62	48
6	27	0	1		144	104
6	28	0	1		204	178
6	29	0	1	L	61	62
6	30	0	1		395	308
6	31	0	1		211	174
6	32	0	1	L	67	80
6	33	0	1	L	68	53
6	34	0	1	L	63	37
6	35	0	1		86	109
6	36	0	1		107	100
6	37	0	1	L	72	30
6	38	0	1		70	71
6	39	0	1	L	69	37
6	40	0	1	L	65	73
6	41	0	1	L	76	90
6	42	0	1		200	159
6	43	0	1		219	204
6	44	0	1	L	69	79
6	45	0	1	L	77	75
6	46	0	1	L	68	25
6	47	0	1	L	73	72
6	48	0	1	L	70	54
6	49	0	1	L	82	76
6	50	0	1		106	110
6	51	0	1	L	73	37
6	52	0	1		174	200
6	53	0	1		191	110
6	54	0	1	L	73	61
6	55	0	1	L	75	64
6	56	0	1	L	70	74
6	57	0	1	L	69	66
6	58	0	1	L	86	65
6	59	0	1	L	76	36
6	60	0	1	L	77	72
6	61	0	1	L	78	22
6	62	0	1	L	75	55
6	63	0	1	L	82	91
6	64	0	1		122	119
6	65	0	1	L	111	134
6	66	0	1	L	77	73
6	67	0	1	L	76	42
6	68	0	1	L	74	5
6	69	0	1	L	80	55
6	70	0	1	L	81	40
6	71	0	1	L	89	58
6	72	0	1	L	82	44
6	73	0	1	L	96	21
6	74	0	1	L	99	93
6	75	0	1	L	93	58
6	76	0	1	L	89	61
6	77	0	1	L	85	69
6	78	0	1	L	91	107
7	74	0	1	L	95	93
7	73	0	1	L	83	50
7	72	0	1	L	85	46
7	71	0	1	L	87	73
7	70	0	1	L	83	40
7	69	0	1	L	85	67
7	68	0	1	L	84	52
7	67	0	1	L	82	96
7	66	0	1	L	69	44
7	65	0	1	L	83	69
7	64	0	1	L	93	79
7	63	0	1	L	93	105
7	62	0	1	L	96	53
7	61	0	1	L	86	75
7	60	0	1	L	81	66
7	59	0	1	L	76	70
7	58	0	1	L	77	66
7	57	0	1	L	81	16
7	56	0	1	L	80	36
7	55	0	1	L	79	77
7	54	0	1		124	113
7	53	0	1		150	133
7	52	0	1	L	86	94
7	51	0	1	L	75	61
7	50	0	1	L	77	42
7	49	0	1	L	79	67
7	48	0	1	L	71	39
7	47	0	1		91	71
7	46	0	1	L	75	74
7	45	0	1		81	76
7	44	0	1	L	72	52
7	43	0	1	L	76	80
7	42	0	1		190	137
7	41	0	1		218	194
7	40	0	1		85	72
7	39	0	1		125	121
7	38	0	1	L	74	90
7	37	0	1	L	67	67
7	36	0	1	L	66	72
7	35	0	1	L	73	22
7	34	0	1	L	69	49
7	33	0	1	L	69	64
7	32	0	1		188	135
7	31	0	1		158	136
7	30	0	1		73	86
7	29	0	1	L	62	63
7	28	0	1	L	67	52
7	27	0	1	L	72	56
7	26	0	1	L	71	44
7	25	0	1		113	133
7	24	0	1		137	141
7	23	0	1	L	70	80
7	22	0	1	L	60	65
7	21	0	1		89	95
7	20	0	1		194	189
7	19	0	1		282	258
7	18	0	1		80	72
7	17	0	1		168	196
7	16	0	1		88	90

H	K	L	GRP		FC	FC
7	15	0	1	L	65	36
7	14	0	1	L	68	48
7	13	0	1	L	65	44
7	12	0	1		98	102
7	11	0	1		111	122
7	10	0	1		144	141
7	9	0	1		73	90
7	8	0	1	L	69	54
7	7	0	1	L	68	46
7	6	0	1	L	63	80
7	5	0	1		102	103
7	4	0	1		79	63
7	3	0	1		221	230
7	2	0	1		236	205
7	1	0	1		114	103
7	0	0	1	L	71	62
8	0	0	1		78	74
8	1	0	1		75	93
8	2	0	1	L	66	56
8	3	0	1	L	65	61
8	4	0	1	L	64	42
8	5	0	1		84	84
8	6	0	1	L	73	78
8	7	0	1		109	109
8	8	0	1		177	163
8	9	0	1		216	193
8	10	0	1		109	100
8	11	0	1	L	69	76
8	12	0	1		132	100
8	13	0	1		188	181
8	14	0	1		99	101
8	15	0	1		117	90
8	16	0	1	L	70	32
8	17	0	1	L	68	63
8	18	0	1	L	70	70
8	19	0	1	L	72	62
8	20	0	1		103	99
8	21	0	1		117	103
8	22	0	1	L	70	61
8	23	0	1	L	73	70
8	24	0	1	L	65	20
8	25	0	1	L	63	72
8	26	0	1	L	70	42
8	27	0	1	L	81	89
8	28	0	1		110	95
8	29	0	1		119	116
8	30	0	1		166	164
8	31	0	1		152	159
8	32	0	1	L	84	82
8	33	0	1		70	50
8	34	0	1	L	81	82
8	35	0	1		125	124
8	36	0	1	L	77	59
8	37	0	1	L	77	78
8	38	0	1	L	71	61
8	39	0	1	L	74	35
8	40	0	1	L	81	77
8	41	0	1	L	79	88
8	42	0	1		123	131
8	43	0	1	L	88	86
8	44	0	1	L	80	49
8	45	0	1	L	73	52
8	46	0	1	L	78	16
8	47	0	1	L	85	68
8	48	0	1	L	86	72
8	49	0	1		92	82
8	50	0	1		87	70
8	51	0	1	L	94	88
8	52	0	1	L	90	107
8	53	0	1	L	93	95
8	54	0	1	L	78	79
8	55	0	1	L	81	28
8	56	0	1	L	82	88
8	57	0	1	L	81	73
8	58	0	1	L	80	48
8	59	0	1	L	84	62
8	60	0	1	L	87	63
8	61	0	1	L	83	43
8	62	0	1	L	89	59
8	63	0	1	L	91	101
8	64	0	1	L	98	122
8	65	0	1	L	96	64
8	66	0	1	L	89	67
8	67	0	1	L	82	41
8	68	0	1	L	85	20
8	69	0	1	L	88	60
8	70	0	1	L	88	65
9	64	0	1	L	97	49
9	63	0	1	L	88	57
9	62	0	1		108	90
9	61	0	1	L	89	60
9	60	0	1	L	91	64
9	59	0	1	L	88	85
9	58	0	1	L	88	70
9	57	0	1	L	82	18
9	56	0	1	L	87	45
9	55	0	1	L	83	26
9	54	0	1	L	90	55
9	53	0	1	L	95	77
9	52	0	1	L	88	101
9	51	0	1	L	82	53
9	50	0	1	L	87	43
9	49	0	1	L	89	56
9	48	0	1	L	80	81
9	47	0	1	L	78	17
9	46	0	1	L	92	108
9	45	0	1	L	87	102
9	44	0	1	L	77	38
9	43	0	1	L	82	81
9	42	0	1	L	90	109
9	41	0	1	L	89	85
9	40	0	1	L	101	128
9	39	0	1	L	78	57
9	38	0	1	L	85	75
9	37	0	1	L	73	70
9	36	0	1	L	74	74
9	35	0	1	L	78	6
9	34	0	1	L	78	58
9	33	0	1	L	74	21
9	32	0	1	L	82	74
9	31	0	1		85	78
9	30	0	1	L	69	80
9	29	0	1		87	65
9	28	0	1	L	75	45
9	27	0	1	L	72	34
9	26	0	1	L	85	94
9	25	0	1	L	68	38
9	24	0	1		177	154
9	23	0	1		126	122
9	22	0	1	L	72	71
9	21	0	1		130	106
9	20	0	1		130	159
9	19	0	1		113	103
9	18	0	1		140	190
9	17	0	1	L	71	44
9	16	0	1		79	72
9	15	0	1	L	70	48
9	14	0	1	L	67	71
9	13	0	1	L	63	21
9	12	0	1	L	74	77
9	11	0	1	L	70	74
9	10	0	1		88	84
9	9	0	1	L	74	48
9	8	0	1	L	66	68
9	7	0	1	L	71	47
9	6	0	1	L	65	58
9	5	0	1	L	65	16
9	4	0	1	L	79	114
9	3	0	1	L	79	85
9	2	0	1		185	175
9	1	0	1		91	119
9	0	0	1	L	74	88
10	0	0	1	L	83	94

H	K	L	GRP		FO	FI
10	1	0	1	L	82	69
10	2	0	1	L	70	24
10	3	0	1	L	74	69
10	4	0	1	L	74	25
10	5	0	1	L	70	28
10	6	0	1	L	74	35
10	7	0	1	L	81	103
10	8	0	1	L	72	46
10	9	0	1	L	86	123
10	10	0	1	L	88	97
10	11	0	1	L	75	80
10	12	0	1	L	88	110
10	13	0	1	L	95	128
10	14	0	1	L	67	22
10	15	0	1	L	81	90
10	16	0	1	L	83	47
10	17	0	1	L	73	34
10	18	0	1	L	68	42
10	19	0	1	L	73	84
10	20	0	1	L	73	37
10	21	0	1	L	80	61
10	22	0	1		86	65
10	23	0	1	L	74	63
10	24	0	1	L	68	8
10	25	0	1	L	77	71
10	26	0	1	L	83	50
10	27	0	1	L	80	41
10	28	0	1	L	78	42
10	29	0	1	L	91	109
10	30	0	1	L	79	62
10	31	0	1	L	88	90
10	32	0	1	L	84	74
10	33	0	1	L	78	75
10	34	0	1	L	91	106
10	35	0	1		134	100
10	36	0	1	L	78	20
10	37	0	1	L	81	74
10	38	0	1	L	84	56
10	39	0	1	L	85	56
10	40	0	1	L	84	41
10	41	0	1	L	82	95
10	42	0	1	L	85	48
10	43	0	1	L	83	52
10	44	0	1	L	83	14
10	45	0	1	L	76	39
10	46	0	1	L	80	19
10	47	0	1	L	84	69
10	48	0	1	L	84	83
10	49	0	1	L	93	53
10	50	0	1	L	79	49
10	51	0	1	L	99	102
10	52	0	1	L	84	91
10	53	0	1	L	90	58
10	54	0	1	L	85	57
10	56	0	1	L	82	47
10	57	0	1	L	93	94
10	58	0	1	L	92	79
10	58	0	1	L	91	18
11	50	0	1	L	87	57
11	49	0	1	L	93	50
11	48	0	1	L	87	56
11	47	0	1	L	89	91
11	46	0	1	L	89	86
11	45	0	1	L	93	84
11	44	0	1	L	87	68
11	43	0	1	L	88	57
11	42	0	1	L	84	56
11	41	0	1	L	77	26
11	40	0	1	L	89	97
11	39	0	1	L	81	61
11	38	0	1	L	79	30
11	37	0	1	L	85	72
11	36	0	1	L	81	76
11	35	0	1	L	78	1
11	34	0	1	L	80	41
11	33	0	1	L	83	49
11	32	0	1	L	83	34
11	31	0	1	L	76	17
11	30	0	1	L	79	93
11	29	0	1	L	81	31
11	28	0	1	L	80	39
11	27		1	L	84	71
11	26	0	1	L	79	54
11	25	0	1	L	81	50
11	24	0	1	L	81	96
11	23	0	1	L	92	93
11	22	0	1	L	76	76
11	21	0	1	L	81	74
11	20	0	1	L	87	79
11	19	0	1	L	79	29
11	18	0	1	L	87	93
11	17	0	1	L	78	55
11	16	0	1	L	74	16
11	15	0	1	L	77	22
11	14	0	1	L	73	89
11	13	0	1	L	77	18
11	12	0	1	L	77	43
11	11	0	1	L	79	74
11	10	0	1	L	76	42
11	9	0	1	L	76	19
11	8	0	1	L	80	90
11	7	0	1	L	76	19
11	6	0	1	L	75	20
11	5	0	1	L	80	65
11	4	0	1		91	68
11	3	0	1	L	79	36
11	2	0	1		103	93
11	1	0	1	L	93	96
11	0	0	1	L	83	83
12	0	0	1		90	83
12	1	0	1	L	83	98
12	2	0	1	L	77	15
12	3	0	1	L	78	83
12	4	0	1	L	77	25
12	5	0	1	L	73	23
12	6	0	1	L	79	59
12	7	0	1	L	82	61
12	8	0	1	L	76	22
12	9	0	1	L	77	64
12	10	0	1	L	86	66
12	11	0	1		95	99
12	12	0	1	L	92	78
12	13	0	1	L	86	75
12	14	0	1	L	82	43
12	15	0	1	L	84	29
12	16	0	1	L	78	63
12	17	0	1	L	79	46
12	18	0	1	L	80	17
12	19	0	1	L	80	86
12	20	0	1	L	80	12
12	21	0	1	L	86	47
12	22	0	1	L	84	68
12	23	0	1	L	87	48
12	24	0	1	L	79	4
12	25	0	1	L	81	72
12	26	0	1	L	82	61
12	27	0	1	L	82	8
12	28	0	1		92	57
12	29	0	1	L	85	81
12	30	0	1	L	79	7
12	31	0	1	L	78	48
12	32	0	1	L	89	54
12	33	0	1	L	90	85
12	34	0	1	L	100	76
12	35	0	1	L	91	78
12	36	0	1	L	89	59
12	37	0	1	L	84	30
12	38	0	1	L	81	57
12	39	0	1	L	85	56
13	23	0	1	L	90	55
13	22	0	1	L	85	84
13	21	0	1	L	84	40
13	20	0	1	L	82	43

1971*a*). The identical appearance of zero and upper level Weissenberg photographs taken about c indicated that atoms were to be found predominantly in the (001) planes. However, the Laue symmetry and systematic absences in spectra indicated space groups that could not be used to successfully interpret the Patterson function. It was therefore decided to solve the structure in projection using the small number of rectangular primitive plane groups. As with the $Ta_{30}W_2O_{81}$ structure, the plane groups that permitted a satisfactory refinement of the metal atom positions were *pm* and *pg*, and the structure of the asymmetric unit ($a \times b/2 \times c$) was found to be virtually the same for either plane group *pm* or *pg*.

Refinement was carried out in the plane group *pm*. Positional and thermal parameters were varied in the full-matrix least-squares cycles for all atoms other than those oxygen atoms which projected onto metal atoms. Positional parameters for these atoms remained at the values determined from difference Fourier syntheses, and an isotropic temperature factor, $B = 0{\cdot}7$ Å^2, was assigned on the basis of the average of the remaining oxygen temperature factors. Justification for anisotropic thermal parameters for the metal atoms only was obtained from the appearance of difference Fourier syntheses and by the use of statistical tests (Hamilton, 1965).

Standard deviations, σF_o, were assigned to F_o data on the basis of counting statistics and a weighting scheme was used (Stephenson & Roth, 1971*a*) to

Table 2. *Positional and thermal parameters for the compound* L-Ta_2O_5

Standard deviations are given in brackets and the form of the anisotropic thermal ellipsoids is $\exp[-(\beta_{11}h^2 + \beta_{22}k^2 + 2\beta_{12}hk)]$. Atoms O(17) to O(28) have z parameters of $\frac{1}{2}$; the remaining atoms have z parameters of zero. Oxygen atoms O(5), O(30), O(31) and O(33) have population parameters of 0·25 while O(29) and O(32) have population parameters of 0·75.

	x/a	y/b	$\beta_{11} \times 10^4$ or B	$\beta_{22} \times 10^5$	$\beta_{12} \times 10^5$
M(1)	0·0000	0·0000	−34 (6)	4 (2)	0
M(2)	0·6784 (15)	0·5000	60 (13)	20 (4)	0
M(3)	0·0655 (12)	0·08622 (16)	91 (11)	2 (2)	−58 (14)
M(4)	0·0558 (9)	0·18372 (14)	44 (7)	8 (2)	−6 (9)
M(5)	0·0674 (12)	0·27489 (18)	80 (11)	9 (2)	−6 (13)
M(6)	0·1610 (11)	0·36266 (20)	69 (10)	20 (3)	72 (12)
M(7)	0·1094 (12)	0·45071 (29)	122 (17)	38 (5)	176 (23)
M(8)	0·5917 (13)	0·41238 (23)	64 (9)	21 (3)	−79 (14)
M(9)	0·5915 (9)	0·31715 (15)	−9 (7)	6 (1)	53 (7)
M(10)	0·6180 (13)	0·22243 (21)	152 (18)	3 (2)	−10 (12)
M(11)	0·5220 (9)	0·13771 (14)	64 (9)	1 (1)	−114 (10)
M(12)	0·5488 (11)	0·04624 (16)	63 (11)	5 (2)	−31 (12)
O(1)	0·648 (8)	0·0000	−0·4 (0·6)		
O(2)	0·251 (11)	0·0290 (11)	0 8 (1 0)		
O(3)	0 882 (16)	0 0457 (33)	2 1 (1·6)		
O(4)	0·402 (11)	0·0923 (24)	0·7 (0·9)		
O(5)	0·798 (36)	0·1090 (82)	0·1 (3·1)		
O(6)	0·189 (13)	0·1354 (26)	1·1 (1·1)		
O(7)	0·398 (11)	0·1886 (24)	0·8 (1·1)		
O(8)	0·978 (9)	0·2265 (19)	0·7 (1·0)		
O(9)	0·400 (11)	0·2668 (21)	0·7 (1·0)		
O(10)	0·732 (9)	0·2775 (18)	0·2 (0·7)		
O(11)	0·283 (12)	0·3152 (28)	1·1 (1·1)		
O(12)	0·466 (14)	0·3655 (23)	1·1 (1·1)		
O(13)	0·275 (11)	0·4076 (23)	0·4 (1·0)		
O(14)	0·398 (6)	0·4681 (14)	−0·2 (0·5)		
O(15)	0·773 (8)	0·4540 (15)	−0·3 (0·6)		
O(16)	0·021 (14)	0·5000	0·6 (1·6)		
O(17)	0·028	0·0000	0·7		
O(18)	0·650	0·5000	0·7		
O(19)	0·090	0·0830	0·7		
O(20)	0·090	0·1775	0·7		
O(21)	0·030	0·2780	0·7		
O(22)	0·160	0·3610	0·7		
O(23)	0·100	0·4500	0·7		
O(24)	0·560	0·0480	0·7		
O(25)	0·512	0·1390	0·7		
O(26)	0·620	0·2230	0·7		
O(27)	0·580	0·3115	0·7		
O(28)	0·582	0·4133	0·7		
O(29)	0·860	0·1300	0·7		
O(30)	0 770	0 1725	0·7		
O(31)	0·900	0·3285	0·7		
O(32)	0·830	0·3675	0·7		
O(33)	0·870	0·3890	0·7		

minimize the effects of uncertainties in the large F_o values brought about by extinction. The final R_1 value for all $hk0$ data is 0·088.

Positional and thermal parameters for L-Ta_2O_5, as well as corresponding standard deviations estimated from the inverse matrix, are given in Table 2. Bond distances and angles, together with estimated standard deviations, are given in Table 3.

Table 3. *Bond distances* (Å) *and angles* (°) *for the compound* L-Ta_2O_5

Standard deviations are given in brackets and refer to the least significant digits. Primed atoms are related by $x, \bar{y}, z$.

M(1) Pentagonal bipyramid	
M(1) –O(1)	2·19 (05) (1)
–O(2)	1·95 (08) (2)
–O(3)	2·00 (13) (2)
–O(17)	1·96 (15) (2)
O(1)—O(3)	2·38 (13) (2)
O(3)—O(2)	2·39 (13) (2)
O(2)—O(2′)	2·33 (13) (1)
O(17)–O(1)	3·07 (06) (2)
–O(2)	2·67 (07) (4)
–O(3)	2·85 (11) (4)
O(1)—O(3)—O(2)	111 (6) (2)
O(3)—O(2)—O(2′)	107 (5) (2)
O(3)—O(1)—O(3′)	103 (4) (1)
M(2) Pentagonal bipyramid	
M(2) –O(14)	2·18 (05) (2)
–O(15)	1·95 (06) (2)
–O(16)	2·14 (09) (1)
–O(18)	1·96 (15) (2)
O(14)–O(15)	2·42 (07) (2)
O(15)–O(16)	2·42 (08) (2)
O(14)–O(14′)	2·57 (08) (1)
O(18)–O(16)	3·03 (09) (2)
–O(15)	2·81 (07) (4)
–O(14)	2·82 (06) (4)
O(14)–O(15)–O(16)	116 (4) (2)
O(15)–O(14)–O(14′)	104 (3) (2)
O(15)–O(16)–O(15′)	101 (4) (1)
M(3) Pentagonal bipyramid	
M(3) –O(2)	2·60 (09) (1)
–O(3)	1·98 (13) (1)
–O(4)	2·13 (07) (1)
–O(5)	1·92 (26) (1)
–O(6)	2·14 (11) (1)
–O(19)	1·97 (15) (2)
O(2)—O(3)	2·39 (13) (1)
O(3)—O(5)	2·67 (36) (1)
O(5)—O(6)	2·62 (26) (1)
O(6)—O(4)	2·21 (13) (1)
O(4)—O(2)	2·73 (13) (1)
O(19)–O(2)	3·11 (09) (2)
–O(3)	2·77 (10) (2)
–O(4)	2·79 (07) (2)
–O(5)	2·89 (20) (2)
–O(6)	2·95 (10) (2)
O(2)—O(3)—O(5)	118 (7)
O(3)—O(5)—O(6)	101 (9)
O(5)—O(6)—O(4)	105 (8)
O(6)—O(4)—O(2)	122 (4)
O(4)—O(2)—O(3)	94 (5)
M(4) Octahedron	
M(4) –O(6)	2·14 (10) (1)
–O(7)	2·17 (07) (1)

Table 3 (*cont.*)

M(4)—O(8)	1·78 (08) (1)
–O(30)	1·83 (06) (1)
–O(20)	1·98 (15) (2)
O(6)—O(7)	2·52 (14) (1)
O(7)—O(8)	3·05 (10) (1)
O(8)—O(30)	2·54 (11) (1)
O(30)–O(6)	3·02 (11) (1)
O(20)–O(6)	2·67 (09) (2)
–O(7)	2·79 (07) (2)
–O(8)	2·87 (08) (2)
–O(30)	2·80 (06) (2)
O(6)—O(7)—O(8)	89 (4)
O(7)—O(8)—O(30)	91 (3)
O(8)—O(30)–O(6)	90 (2)
O(30)–O(6)—O(7)	91 (4)
M(5) Octahedron	
M(5) –O(8)	2·05 (08) (1)
–O(9)	2·09 (07) (1)
–O(10)	2·11 (06) (1)
–O(11)	2·11 (10) (1)
–O(21)	1·97 (15) (2)
O(9)—O(11)	2·07 (14) (1)
O(11) O(10)	3·19 (11) (1)
O(10)–O(8)	2·59 (10) (1)
O(8)—O(9)	3·11 (10) (1)
O(21)–O(8)	2·88 (08) (2)
–O(9)	3·05 (07) (2)
–O(10)	2·71 (06) (2)
–O(11)	2·93 (10) (2)
O(8)—O(9)—O(11)	101 (4)
O(9)—O(11)–O(10)	81 (3)
O(11)–O(10)–O(8)	84 (4)
O(10)–O(8)—O(9)	94 (3)
M(6) Pentagonal bipyramid	
M(6) –O(11)	2·08 (11) (1)
–O(12)	1·94 (09) (1)
–O(13)	1·95 (09) (1)
–O(31)	2·14 (07) (1)
–O(33)	2·11 (07) (1)
–O(22)	1·96 (15) (2)
O(11)–O(12)	2·40 (14) (1)
O(12)–O(13)	2·04 (13) (1)
O(13)–O(33)	2·65 (10) (1)
O(33)–O(31)	2·46 (11) (1)
O(31)–O(11)	2·46 (10) (1)
O(22)–O(11)	2·80 (10) (2)
–O(12)	2·76 (08) (2)
–O(13)	2·81 (09) (2)
–O(31)	2·86 (07) (2)
–O(33)	2·90 (07) (2)
O(11)–O(12)–O(13)	114 (5)
O(12)–O(13)–O(33)	110 (5)
O(13)–O(33)–O(31)	102 (3)
O(33)–O(31)–O(11)	107 (4)
O(31)–O(11)–O(12)	106 (5)
M(7) Octahedron	
M(7) –O(13)	2·02 (09) (1)
–O(14)	1·93 (05) (1)
–O(15)	2·12 (05) (1)
–O(16)	2·08 (03) (1)
–O(23)	1·96 (10) (2)
O(13)–O(14)	2·57 (11) (1)
O(14)–O(16)	2·69 (09) (1)
O(15)–O(13)	3·12 (10) (1)
O(16)–O(15)	2·42 (08) (1)
O(23)–O(13)	2·83 (08) (2)
–O(14)	2·80 (06) (2)

Table 3 (*cont.*)

O(23)-O(15)	2·83 (06) (2)
-O(16)	2·86 (06) (2)
O(13)-O(14)-O(16)	101 (2)
O(14)-O(16)-O(15)	101 (2)
O(16)-O(15)-O(13)	90 (2)
O(15)-O(13)-O(14)	68 (3)
M(8) Pentagonal bipyramid	
M(8) -O(12)	1·99 (10) (1)
-O(13)	1·97 (07) (1)
-O(14)	2·56 (06) (1)
-O(15)	2·04 (06) (1)
-O(33)	1·99 (07) (1)
-O(28)	1·96 (10) (2)
O(12)-O(13)	2·14 (13) (1)
O(13)-O(14)	2·57 (11) (1)
O(14)-O(15)	2·42 (07) (1)
O(15)-O(33)	2·71 (10) (1)
O(33)-O(12)	2·66 (11) (1)
O(28)-O(12)	2·80 (09) (2)
-O(13)	2·74 (07) (2)
-O(14)	3·18 (08) (2)
-O(15)	2·83 (07) (2)
-O(33)	2·83 (07) (2)
O(12)-O(13)-O(14)	126 (4)
O(13)-O(14)-O(15)	94 (3)
O(14)-O(15)-O(33)	116 (3)
O(15)-O(33)-O(12)	91 (2)
O(33)-O(12)-O(13)	107 (5)
M(9) Octahedron	
M(9) -O(10)	1·83 (07) (1)
-O(11)	1·92 (08) (1)
-O(12)	2·16 (10) (1)
-O(31)	1·99 (06) (1)
-O(27)	1·97 (10) (2)
O(10)-O(11)	3·19 (11) (1)
O(11)-O(12)	2·40 (14) (1)
O(12)-O(31)	3·11 (12) (1)
O(31)-O(10)	2·32 (11) (1)
O(27)-O(10)	2·57 (07) (2)
-O(11)	2·70 (07) (2)
-O(12)	3·06 (10) (2)
-O(31)	2·88 (07) (2)
O(10)-O(11)-O(12)	89 (4)
O(11)-O(12)-O(31)	89 (4)
O(12)-O(31)-O(10)	93 (3)
O(31)-O(10)-O(11)	89 (3)

Table 3 (*cont.*)

M(10) Pentagonal bipyramid	
M(10) -O(7)	1·95 (09) (1)
-O(8)	2·26 (06) (1)
-O(9)	2·26 (08) (1)
-O(10)	2·33 (08) (1)
-O(30)	2·24 (08) (1)
-O(26)	1·95 (10) (2)
O(7)—O(9)	3·19 (13) (1)
O(9)—O(10)	2·12 (09) (1)
O(10)—O(8)	2·59 (10) (1)
O(8)—O(30)	2·54 (11) (1)
O(26)—O(7)	2·77 (08) (2)
-O(8)	2·97 (07) (2)
-O(9)	2·99 (08) (2)
-O(10)	3·03 (08) (2)
-O(30)	2·98 (08) (2)
O(7)—O(9)—O(10)	101 (4)
O(9)—O(10)-O(8)	115 (4)
O(10)—O(8)—O(30)	112 (4)
O(8)—O(30)-O(7)	105 (4)
O(30)—O(7)—O(9)	106 (4)
M(11) Pentagonal bipyramid	
M(11) -O(4)	1·99 (10) (1)
-O(5)	2·06 (26) (1)
-O(6)	2·08 (09) (1)
-O(7)	2·19 (10) (1)
-O(30)	2·09 (07) (1)
-O(25)	1·96 (10) (2)
O(4)—O(5)	2·61 (25) (1)
O(5)—O(30)	2·50 (34) (1)
O(30)—O(7)	2·41 (10) (1)
O(7)—O(6)	2·52 (14) (1)
O(6)—O(4)	2·21 (13) (1)
O(25)—O(4)	2·81 (09) (2)
-O(5)	2·90 (20) (2)
-O(6)	2·81 (08) (2)
-O(7)	2·88 (09) (2)
-O(30)	2·87 (07) (2)
O(4)—O(6)—O(7)	111 (4)
O(6)—O(7)—O(30)	106 (5)
O(7)—O(30)-O(5)	110 (6)
O(30)—O(5)—O(4)	102 (10)
O(5)—O(4)—O(6)	110 (8)
M(12) Octahedron	
M(12) -O(1)	1·98 (02) (1)
-O(2)	1·99 (08) (1)

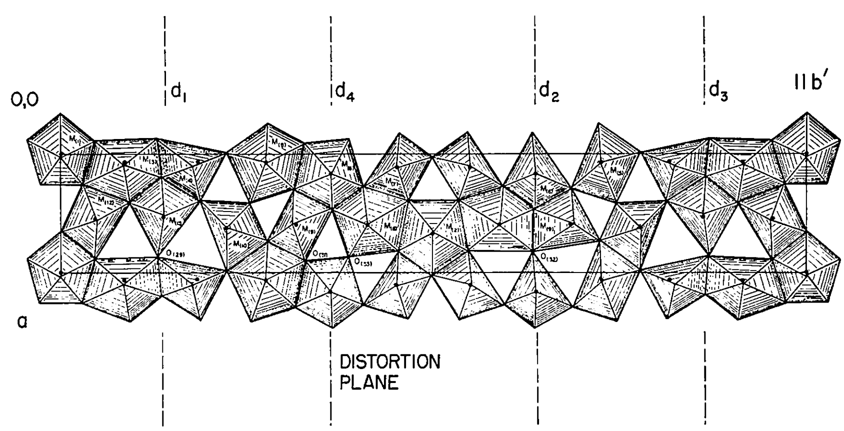

Fig. 1. A (001) projection of the structure of L-Ta_2O_5. There are three distortion planes in this unit cell located at d_1, d_2 and d_3. The fourth position at d_4 is related by symmetry but is not used in this unit cell. Black dots represent metal atoms and shaded areas oxygen coordination polyhedra.

Table 3 (*cont.*)

M(12)–O(3)	2·10 (10) (1)
–O(4)	2·07 (09) (1)
–O(24)	1·96 (08) (2)
O(1)—O(2)	2·75 (09) (1)
O(2)—O(4)	2·73 (13) (1)
O(4)—O(3)	3·02 (12) (1)
O(3)—O(1)	2·38 (13) (1)
O(24)—O(1)	2·81 (06) (2)
–O(2)	2·86 (07) (2)
–O(3)	2·82 (09) (2)
–O(4)	2·82 (09) (2)
O(1)—O(2)—O(4)	94 (3)
O(2)—O(4)—O(3)	81 (3)
O(4)—O(3)—O(1)	82 (3)
O(3)—O(1)—O(2)	103 (3)

Description of the structure

The ideal structure for L-Ta_2O_5 can be generated from a chain of 8 edge-sharing pentagons which is regularly folded in the manner desribed by Roth & Stephenson (1969). The plane group of the (001) projection of this ideal structure is *pgm*, and the ideal unit cell contains 22 metal atoms and 58 oxygen atoms.

The real structure of L-Ta_2O_5 differs from the ideal structure by the way in which certain pentagonal bipyramids accommodate the distortions imposed upon them in the ideal structure by the folding process. This process can involve a reduction in the coordination number of some metal atoms. The real unit cell of L-Ta_2O_5 contains 22 metal atoms and 55 oxygen atoms; therefore three metal atoms per unit cell reduce the coordination number from seven (in the ideal case) to six (in the real case).

In the structure of $Ta_{22}W_4O_{67}$ (Stephenson & Roth, 1971*a*), the location of such a reduction, or a distortion plane, was associated with a splitting of one of the oxygen peaks, whereas in the structure of $Ta_{30}W_2O_{81}$ (Stephenson & Roth, 1971*b*), the distortion planes were located where oxygen peak heights were lower than average. In the structure of L-Ta_2O_5, both of these identifying features are observed: two atomic sites, O(30) and O(31), which are normally fully occupied in the ideal structure are only partially occupied in the real structure. Also, atomic sites O(5) and O(33) which would be single peaks in the ideal structure of Ta_2O_5, appear as doublets in the real structure *viz.* O(5), O(29) and O(33), O(32).

Consider the environment of tantalum atom M(11). When O(5) and O(30) are occupied, M(11) has pentagonal bipyramidal coordination. When O(5) and O(30) are not occupied but O(29) is occupied, M(11) has a distorted octahedral configuration. A similar argument

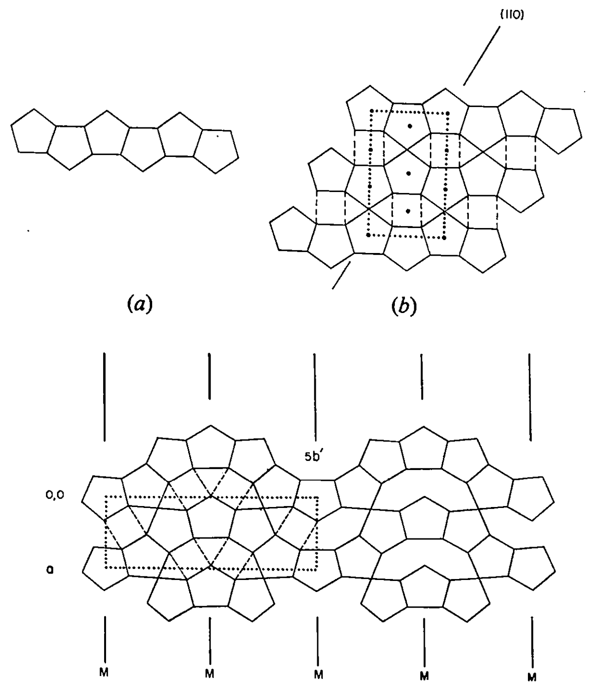

Fig. 2. (*a*) A chain of edge-sharing regular pentagons – a basic building unit in the representation of ideal structures of phases in the Ta_2O_5–WO_3 system. (*b*) The ideal M_6O_{16} structure formed by a fusion of three chains, showing the formation of octahedral sites between adjacent chains. Dots represent metal atoms with superimposed oxygen atoms. If this structure is reflected about the (110) plane a 'herring-bone weave' effect is produced [as in Fig. 2(*c*)] with a subsequent reduction in the oxygen:metal ratio. (*c*) The ideal structure of $M_{10}O_{26}$, the smallest basic structure, consisting of five UO_3-type subcells (each of length b').

Table 4. *Correlation coefficients, ϱ_{ij}, for metal–metal positional parameter interactions*

x_i–x_j type interactions are shown below the ϱ_{ii} diagonal while y_i–y_j type interactions are found above this diagonal. There are no values of ϱ_{ij} greater than 0·58.

	2	3	4	5	6	7	8	9	10	11	12
2	1·0	—	—	—	—	—	—	—	—	—	—
3	0·06	1·0	−0·01	0·19	0·11	−0·14	0·30	−0·01	0·18	0·10	0·03
4	0·24	0·27	1·0	−0·13	−0·09	0·38	0·11	0·20	0·02	0·18	0·12
5	0·15	0·17	0·09	1·0	0·22	−0·24	0·06	0·25	0·31	−0·11	−0·25
6	0·19	0·10	0·42	0·08	1·0	0·05	−0·01	0·07	0·12	0·41	0·15
7	0·23	0·03	0·10	0·30	0·04	1·0	0·07	0·16	−0·16	0·32	0·04
8	0·03	0·43	0·54	−0·03	0·38	0·10	1·0	−0·10	0·21	0·12	−0·16
9	0·20	0·15	0·40	0·34	0·34	0·07	−0·02	1·0	0·13	−0·17	0·05
10	0·06	0·13	0·49	0·16	0·35	−0·01	0·33	0·25	1·0	0·12	−0·34
11	0·17	0·38	0·58	0·11	0·19	0·12	0·42	0·54	0·30	1·0	0·19
12	0·41	0·20	0·30	0·36	0·14	0·52	0·17	0·25	0·01	0·25	1·0

applies to M(6), which has pentagonal bipyramidal coordination when O(31) and O(33) are both occupied and distorted octahedral coordination when O(32) is occupied. Since there are two asymmetric units in the complete unit cell, there are four available sites per unit cell for distortion plane locations. The three distortion planes are therefore statistically distributed over these four locations. The unit cell of L-Ta_2O_5 (Fig. 1) is therefore an average unit cell in which the distortion planes are shown as d_1, d_2, and d_3. The remaining location d_4 is not utilized in this unit cell, although it would be used in adjacent unit cells. The atomic site occupancies for O(5) and O(29)–O(33), given in Table 2, agree with the observed peak heights.

Correlation coefficients for x–x and y–y type parameter interactions for the metal atoms are given in Table 4 and were calculated by the *ORFLS* (Busing, Martin & Levy, 1962) program. The comparatively low magnitudes of these interactions (maximum ϱ_{ij} value, 0·58) can be attributed to the use of more extensive data to determine and refine the structural parameters.

Thermal equilibration and structural change

Each compound in the series Ta_2O_5–$11Ta_2O_5.4WO_3$ has a structure that is dependent on its thermal history. After extensive heat treatment the structure of any member of the above series reaches its equilibrium state and can no longer be altered by annealing. Details of such thermally equilibrated structures have been published in the preceding papers, and it is now

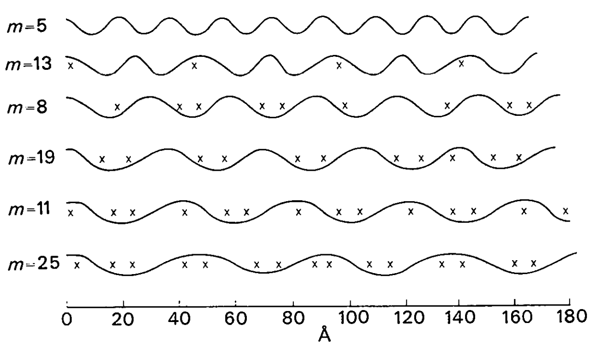

Fig. 3. A schematic representation of the distribution of distortion planes along the **b** direction of some structures that have reached equilibrium. The distortion plane locations are marked with crosses. The multiplicity, m, refers to the number of UO_3-type subcells in the unit cell in which the distortion plane distribution is shown.

possible to discuss the structural changes that occur between the original formation of the substance and its final equilibrated state.

Consider the case of pure Ta_2O_5. Pure Ta_2O_5 can be prepared by heating tantalum metal in air or oxygen at 600°C. Powder photographs of this semi-amorphous Ta_2O_5 resemble those of U_3O_8 and the structure presumably contains chains of pentagonal bipyramids [see Fig. 2(a)] of varying lengths, which have begun to fuse together as shown in Fig. 2(b). Further heating of the substance, just below its transition point, induces crystallization and in order to reduce the oxygen : metal ratio to below 2·667:1, which would be the value if the chains remained linear as in Fig. 2(b), a folding or herring-bone weave dictates the structural trend. This herring-bone weave is obtained by reflecting the structure across the (110) plane. The smallest structural unit in the Ta_2O_5–$11Ta_2O_5.4WO_3$ series is shown in Fig. 2(c). The unit cell, based on 5 UO_3-type subcells, has composition $M_{10}O_{26}$ (where M represents a metal atom).

L-Ta_2O_5 initially displays a reasonably sharp powder photograph with superlattice lines that can be indexed on the basis of a 14 UO_3-type subcell. Prolonged heating for two weeks at 1350°C gradually changes the multiplicity of the unit cell to 11. A reduction towards 8 UO_3-type subcells can only be obtained by adding impurity such as Al_2O_3 or WO_3.

The ideal composition of the 14-subcell structure is $M_{28}O_{74}$. Since the actual composition is $M_{28}O_{70}$ (*i.e.* Ta_2O_5) there will be four distortion planes per unit cell in the real 14-subcell structure, *i.e.* 0·286 distortion planes per subcell. The crystal structure determination of the 11-subcell structure of Ta_2O_5 has shown that there are three distortion planes per unit cell, *i.e.* 0·273 distortion planes per subcell. Thus in changing from a 14-subcell to an 11-subcell structure, Ta_2O_5 has undergone a decrease in the concentration of distortion planes. Some distortions have been annealed out by the heat treatment.

A similar trend is observed with every other member of the Ta_2O_5–$11Ta_2O_5.4WO_3$ series. Any given compound contains more 'long chains' initially than it does after equilibration. For example, the compound $Ta_{22}W_4O_{67}$ is made up of 5 subcell and 8 subcell blocks in the ratio 1:1, and the pentagon chains are respectively 4 and 6 pentagons long in each case. However, before equilibration there is a greater number of 8 subcell blocks than there are 5 subcell blocks, which corresponds to a higher concentration of distortion planes.

Table 5. *Data concerning the distribution of distortion planes along the* [010] *direction*

Compound	Number of subcells	Distance within doublet	Distance between doublets
$11Ta_2O_5.4WO_3$	13	None	47·40 Å
$15Ta_2O_5.2WO_3$	8	7 Å	29·23
$37Ta_2O_5.2WO_3$	19	9	34·78
L-Ta_2O_5	11	6·3	20·24

There is a definite tendency for distortion planes to pair. For the purposes of Table 5, the distances between distortion planes have been measured between the positions that oxygen atoms would have occupied in the fully-oxygenated or (non-existent) ideal structures. Thus distortion planes pair at distance between 6 and 8 ångström units. In addition to these pairs single distortion planes are distributed fairly evenly between the doublets. These can be seen in Fig. 3.

The structural consequences of thermal annealing are as follows:

1. When a member of the series Ta_2O_5–$11Ta_2O_5.4WO_3$ is first formed its structure is made up of a sequence of herring-boned chains of fused pentagons. The linear portions of any chain may contain 4, 6, 8, ..., $2n$ edge-shared pentagons which result in 5, 8, 11, ..., $(3n/2)$–1 basic subcell blocks. Initially, a large number of distortion planes are distributed evenly and mostly in pairs.
2. As (heat) energy is supplied to the system the lengths of the straight portions of the chains are decreased, the number of distortion planes is decreased and the number of pairs of distortion planes is decreased. These features are all interrelated and reflect changes in structure.

Table 5 and Fig. 3 both illustrate that as the oxygen: metal ratio decreases, the concentration of distortion planes increases and therefore the distances between the planes decreases. The planes are distributed mainly in pairs with occasional single planes distributed evenly between the pairs. As the concentration of distortion planes increases, *i.e.* at the high tantala end of the Ta_2O_5–WO_3 system, it is possible to reverse the annealing process and, by slow cooling, increase the number of larger subcell blocks. The region over which this reversal applies in the Ta_2O_5–Al_2O_3 system is slightly larger since this latter system contains higher concentrations of distortion planes than the corresponding regions in the Ta_2O_5–WO_3 system. It appears, therefore, that when distortion planes occur frequently it is possible to pair the odd distortion plane with one introduced by an overall lengthening of the distances between the pairs.

References

BUSING, W. R., MARTIN, K. O. & LEVY, H. A. (1962). *ORFLS, A Fortran Crystallographic Least-Squares Program.* Report ORNL-TM-305, Oak Ridge National Laboratory, Tennessee.

HAMILTON, W. C. (1965). *Acta Cryst.* **18**, 502.

LAGERGREN, S. & MAGNÉLI, A. (1952). *Acta Chem. Scand.* **6**, 444.

LAVES, F. & PETTER, W. (1964). *Helv. Physica Acta*, **32**, 617.

LEHOVIC, K. (1964). *J. Less-Common Metals*, **7**, 397.

MOSER, R. (1965). *Schweiz. min. petrogr. Mitt.* **45**, [1], 35.

ROTH, R. S. & STEPHENSON, N. C. (1969). *The Chemistry of Extended Defects in Non-Metallic Solids.* Amsterdam: North Holland.

ROTH, R. S. & WARING, J. L. (1971). To be published.

STEPHENSON, N. C. & ROTH, R. S. (1971*a*). *Acta Cryst.* B**27**, 1010.

STEPHENSON, N. C. & ROTH, R. S. (1971*b*). *Acta Cryst.* B**27**, 1018.

WARING, J. L. & ROTH. R, S. (1968). *J. Res. Nat. Bur. Stand.* **72**, 175.

Acta Cryst. (1971). B**27**, 1044

X-ray Study of the Structural and Ionic Configuration of the $CoMnCrO_4$ Spinel

BY D. K. KULKARNI AND CHINTAMANI MANDE
Department of Physics, Nagpur University, Nagpur, India

(*Received* 23 *July* 1970)

A new spinel $CoMnCrO_4$ has been synthesized. Its crystal structure has been determined by the powder method. It is found that this compound is cubic with lattice constant $a = 8{\cdot}34 \pm 0{\cdot}02$ Å. The oxygen ion parameter u in the spinel has been calculated from the intensities of various lines in the powder patterns and is found to be $0{\cdot}386 \pm 0{\cdot}002$. The K-absorption edges of cobalt, manganese and chromium have been recorded photographically in this spinel, using a bent crystal X-ray spectrograph. The positions of these edges have been compared with those in some well-known compounds. The comparison shows that the oxidation states of the manganese, chromium and cobalt ions in this spinel are two, three and three respectively. Combining the structural properties and the X-ray spectroscopic results, the charge and site distribution in the spinel is found to be $Mn^{2+}[Co^{3+}Cr^{3+}]\,O_4^{2-}$.

Introduction

The manganite spinels have attracted much attention in recent years because of their wide use in industry. These oxidic spinels have given rise to much discussion (Kshirsagar & Biswas, 1967) as to their valency states and distribution of the cations in the lattice. Precise information about the charge and site distribution is